Available online at www.sciencedirect.com
SCIENCE DIRECT®

Journal of the European Ceramic Society 24 (2004) 2425–2432
www.elsevier.com/locate/jeurceramsoc

Structure and color of $Ni_xA_{1-3x}B_{2x}O_2$ (A = Ti, Sn; B = Sb, Nb) solid solutions

S. Sorlí, M.A. Tena*, J.A. Badenes, J. Calbo, M. Llusar, G. Monrós

Inorganic Chemistry Area, Inorganic and Organic Chemistry Department, Jaume I University, Apd. 224 Castellón 12071, Spain

Received 10 May 2003; received in revised form 23 July 2003; accepted 29 July 2003

Abstract

In this study, $Ni_xTi_{1-3x}B_{2x}O_2$ (B = Sb, Nb; $0 \leqslant x \leqslant 1/3$) and $Ni_{0.1}A_{0.7}B_{0.2}O_2$ (A = Ti, Sn; B = Sb, Nb) compositions were synthesized by the ceramic method and characterized by X-ray diffraction, UV-V spectroscopy and CIELAB (Commission Internationale de l'Eclairage $L^*a^*b^*$) parameters measurements. $Ni_xTi_{1-3x}Sb_{2x}O_2$ ($0 \leqslant x \leqslant 0.10$) and $Ni_xTi_{1-3x}Nb_{2x}O_2$ ($0 \leqslant x \leqslant 0.30$) solid solutions with rutile structure were obtained at 1300 °C/24 h. From $Ni_{0.1}A_{0.7}B_{0.2}O_2$ (A = Ti, Sn; B = Sb, Nb) compositions, a worse yellow color was obtained when A = Sn than when A = Ti. $Ni_xA_{1-3x}B_{2x}O_2$ with A = Ti, B = Nb, $x \leqslant 0.10$ and 1000 °C $\leqslant T \leqslant$ 1200 °C might be established as compositional and fired temperature ranges to obtain yellow ceramic pigments in these systems.

Keywords: Colour; (Ni, Ti, Nb)O_2; (Ni, Ti, Sb)O_2; Rutile; Pigments

1. Introduction

At the moment, the yellow ceramic pigment used industrially is the praseodymium zircon yellow,[1] but it has some drawbacks in the bulk coloration of porcelainized stoneware. Other yellow ceramic pigments used were: yellow of vanadium–zirconia,[2,3] tin–vanadium yellow,[4,5] cadmium yellow and Naples yellow ($Pb_2Sb_2O_7$).[6] Yellow ceramic pigments based on pyrochlore and cordierite matrix have been reported.[7,8] Ishida et al.[7] studied calcium and vanadium codoped pyrochlore, $Ca_xY_{2-x}V_xTi_{2-x}O_7$. It was found to produce a bright and strong yellow color. When applied in calcium-based glaze, this pigment also produced a brighter and stronger yellow color than commercial yellow pigments, such as vanadium–zirconium yellow and vanadium–tin yellow. The pyrochlore pigment in the glaze, however, was decolorized when fired at 1300 °C. Estrada et al.[8] studied a vanadium cordierite pigment. This pigment was synthesised by sol-gel processing. With addition of vanadium pentoxide, a small solid solution region with the high temperature cordierite structure was detected. The composition range of the cordierite solid solution was found to be 4 wt.% chromophore content. Volatilisation of vanadium occurred with increasing temperature. The hue of these compositions was in the yellow region.

There are two yellow ceramic pigments with rutile structure: (Ni,Sb,Ti)O_2 (11-15-4 DCMA, Dry Color Manufacturers Association)[9] and (Ni,Nb,Ti)O_2 (11-16-4 DCMA).[9] Rutile yellow ceramic pigments have been little used in the ceramic industry because bright yellow coloration of these pigments decreases in transparent glazes. The stability of rutile solid solutions with temperature makes these materials potential substitutes of praseodymium zircon yellow ceramic pigment in the bulk coloration of porcelainized stoneware.

Synthesis, structural characterisation, semiconducting properties and magnetic measurements of $Ti_{3(1-x)}M_x$ $M'_{2x}O_6$ (M = Co, Ni; M′ = Sb, Nb) solid solutions were reported by Pico et al.[10–12] These authors established the compositional range for which the rutile structure was maintained ($0.1 \leqslant x \leqslant 0.3$). Samples were prepared from a powdered mixture of TiO_2, $CoCO_3$ or $NiCO_3$ and Sb_2O_5 or Nb_2O_5, in stoichiometric amounts by heating in air from 1423 to 1523 K for 72 h. In these phases, all the cations were randomly distributed in the parent lattice and no cooperative interactions took

* Corresponding author. Tel.: +34-9647-28249; fax: +34-9647-28214.
E-mail address: tena@qio.uji.es (M.A. Tena).

0955-2219/$ - see front matter © 2003 Elsevier Ltd. All rights reserved.
doi:10.1016/j.jeurceramsoc.2003.07.012

place. Coloration of these materials was not included in these studies.

Some works related color with structure in nickel compounds.[13–15] G. R. Rossman et al. studied the origin of the yellow color of Complex Nickel Oxides.[13] Ni^{2+} in sixfold coordination in oxides generally produces green colors. A bright yellow color resulted when Ni^{2+} was in a six-coordinated site significantly distorted from the octahedral symmetry. Increased absorption intensity occurred when the metal ion d–d bands were in proximity to an ultraviolet transfer band. The dependence of color on structure of some organic pigments was investigated by W. Czajkowski et al.[14] Color changes of the products examined were due to interactions between substituents in the phenyl residue and the chelate ring of the pigments. The color and its intensity were determined both by the location and intensity of charge transfer bands of the metal–ligand or ligand–metal type, as well as by intermolecular interactions in the crystalline state. The relation between color and crystal structure in two isomeric dithiophosphatonickel(II) complexes was studied by W. Poll et al.[15] In this study violet or blue solids were obtained.

In DCMA classification[9] there are no similar yellow ceramic pigments with rutile and cassiterite structure. A yellow ceramic pigment with cassiterite structure is $(Sn,V)O_2$ (11-22-4 DCMA), but there is not a ceramic pigment $(Ni,Sn)O_2$ in this classification. TiO_2 (rutile) and SnO_2 (cassiterite) are isostructural oxides with space group $P4_2/mnm$. Croft et al.[16] investigated the $Sn_xTi_{1-x}O_2$ solid solutions and its interaction with V(V), Cr(III), Cr(VI), Mn(II), Fe(III), Co(II), Ni(II), Cu(II) and Sb(III). A continuous SnO_2–TiO_2 solid solution was obtained in the 500–1250 °C temperature range. The splitting into two phases, one tin-rich and the other titanium-rich was obtained by doping with 10 mol% of metal ions. The solid-solution incorporation of SnO_2 into TiO_2 at $\leqslant 25$ mol% SnO_2 increased the opacifying power and reduced significantly the tendency of the TiO_2 to "yellow" when incorporated into glazes.

The aim of this study is to establish the compositional range of $Ni_xA_{1-3x}B_{2x}O_2$ (A = Ti; B = Sb, Nb) rutile solid solutions for which the materials are yellow. The results obtained with the optimal composition will be compared with those obtained when A = Sn.

2. Experimental procedures

Table 1 shows the compositions prepared and their thermal history. In a first step, $Ni_xTi_{1-3x}B_{2x}O_2$ (B = Sb, Nb; $0 \leqslant x \leqslant 1/3$) samples were prepared (thermal history A). From the characterization of these samples, $x = 0.10$ was chosen to compare results of rutile or cassiterite host matrix. Thus, samples of $Ni_{0.1}A_{0.7}B_{0.2}O_2$ (A = Ti, Sn; B = Sb, Nb) were also prepared (thermal history B).

All compositions were prepared by the ceramic method. The starting materials were NiO (Merck), TiO_2 anatase (Panreac), SnO_2 (Panreac), Sb_2O_3 (Panreac) and Nb_2O_5 (Merck) of reagent grade chemical quality. The appropriate amounts of the starting materials were mixed and homogenized in acetone in a planetary ball mill for 15 min. Residual acetone was removed by evaporation. Dried samples were put into refractory crucibles and fired between 800 and 1400 °C for 12 h of soaking times at each temperature.

The resulting materials were examined with a Siemens D5000 X-ray diffractometer to study the development of the crystalline phases at different temperatures. In $Ni_xTi_{1-3x}Nb_{2x}O_2$ and $Ni_{0.1}A_{0.7}B_{0.2}O_2$ (A = Ti, Sn; B = Sb, Nb) fired samples, a structure profile refinement was carried out by the RIETVELD method[17] with the data obtained in the [20–100] °2θ Bragg angle interval. The experimental conditions used were CuK_α radiation, graphite monochromator, 40 kV, 20 mA, 2° divergence slit, 0.06 detector slit, step size of 0.02 °2θ and 10 s for each step. In the refinements the following parameters were refined: a scale factor, two-theta zero, six parameters from the background, unit cell parameters, peak profile parameters using a pseudo-Voigt function, peak asymmetry, FWHW, Lorentzian ratio (eta), positional x-parameters of O and an overall isotropic temperature factor.

UV–V spectroscopy (diffuse reflectance) allows the Ni(II) site in the solid solutions to be studied. A Lambda 2000 Perkin-Elmer spectrophotometer was used to obtain the UV–V–NIR (ultraviolet visible near infrared) spectra in the 200 to 1400 nm range.

CIE $L^*a^*b^*$ colour parameter measurements,[18] conducted with a Perkin-Elmer colorimeter using a standard illuminant D, were used to differenciate the samples in terms of colour. L^* is the lightness axis

Table 1
Prepared compositions

A	B	Composition	Thermal history[a]
Ti	Sb	$Ni_{0.05}Ti_{0.85}Sb_{0.10}O_2$	A
Ti	Sb	$Ni_{0.10}Ti_{0.70}Sb_{0.20}O_2$	A
Ti	Sb	$Ni_{0.20}Ti_{0.40}Sb_{0.40}O_2$	A
Ti	Sb	$Ni_{0.30}Ti_{0.10}Sb_{0.60}O_2$	A
Ti	Sb	$Ni_{1/3}Sb_{2/3}O_2$	A
Ti	Nb	$Ni_{0.05}Ti_{0.85}Nb_{0.10}O_2$	A
Ti	Nb	$Ni_{0.10}Ti_{0.70}Nb_{0.20}O_2$	A
Ti	Nb	$Ni_{0.20}Ti_{0.40}Nb_{0.40}O_2$	A
Ti	Nb	$Ni_{0.30}Ti_{0.10}Nb_{0.60}O_2$	A
Ti	Nb	$Ni_{1/3}Nb_{2/3}O_2$	A
Ti	Sb	$Ni_{0.10}Ti_{0.70}Sb_{0.20}O_2$	B
Ti	Nb	$Ni_{0.10}Ti_{0.70}Nb_{0.20}O_2$	B
Sn	Sb	$Ni_{0.10}Sn_{0.70}Sb_{0.20}O_2$	B
Sn	Nb	$Ni_{0.10}Sn_{0.70}Nb_{0.20}O_2$	B

[a] A: 800, 1000 and 1300 °C. B: 900, 1000, 1100 1200, 1300 and 1400 °C.

Table 2
Crystalline phase evolution with temperature in $Ni_xTi_{1-3x}B_{2x}O_2$ samples

B	x	Raw sample	800 °C/12 h	1000 °C/12 h	1300 °C/12 h
Sb	0.05	A(s), S1(m), N(w),	A(m), R(m), N(vw)	R(m), S2(m)	R(s)
Sb	0.10	S1(s), A(m), N(w)	R(s), N(vw)	R(s)	R(s)
Sb	0.20	S1(s), A(m), N(w)	R(m), S2(m), N(w)	R(s), NT(vw)	R(s), NT(w)
Sb	0.30	S1(s), A(w), N(w)	R(m), S2(m), N(w)	NS(s), S2(w), NT(vw)	NS(s), NT(w)
Sb	1/3	S1(s), N(w)	S2(s), N(w)	NS(s), S2(m), N(w)	NS(s), N(w)
Nb	0.05	A(s), TN(m), N(w)	A(s), TN(w), N(w)	R(s)	R(s)
Nb	0.10	A(s), TN(m), N(w)	A(s), TN(m), N(w)	R(s)	R(s)
Nb	0.20	A(m), TN(m), N(w)	A(m), TN(w), N(w)	R(s), N(w)	R(s)
Nb	0.30	TN(s), N(m), A(w)	HN(s), N(m), A(vw)	NN(s), R(m), N(w)	R(s)
Nb	1/3	TN(s), N(m)	HN(s), N(m)	NN(s), N(w)	NN(s)

Crystalline phases: R = TiO_2 (rutile), A = TiO_2 (anatase), N = NiO, S1 = Sb_2O_3, S2 = Sb_2O_4, NT = $NiTiO_3$, NS = $NiSb_2O_6$ (trirutile), TN = T–Nb_2O_5, HN = H–Nb_2O_5, NN = $NiNb_2O_6$ (orthorhombic).Diffraction peak intensity: s = strong, m = medium, w = weak, vw = very weak.

(black (0) → white (100)), a^* is the green (−) → red (+) axis and b^* is the blue (−) → yellow (+) axis.

Model 2900 MicroMag Alternating Gradient Magnetometer was used to obtain the magnetic response of $Ni_{0.10}A_{0.70}B_{0.20}O_2$ (A = Ti, Sn; B = Sb, Nb) samples at room temperature. This system uses an alternating gradient field to produce a periodic force on a sample placed in a variable o static D. C. field. The sample is mounted on an extension rod attached to a piezoelectric element.

3. Results and discussion

Table 2 shows crystalline phase evolution with temperature in $Ni_xTi_{1-3x}B_{2x}O_2$ (B = Sb, Nb) samples. Rutile is the only phase obtained at 1300 °C, when B = Nb and $0 \leqslant x \leqslant 0.30$. When B = Sb and $x > 0.10$, $NiTiO_3$ is detected together with rutile or $NiSb_2O_6$ (trirutile) crystalline phase. From these results, it might be established the compositional range for which the rutile structure is maintained at 1300 °C. At this temperature, it is $0 \leqslant x \leqslant 0.10$ when B = Sb and it is $0 \leqslant x \leqslant 0.30$ when B = Nb.

Fig. 1 shows the rutile unit cell parameters obtained by the Rietveld method for $Ni_xTi_{1-3x}Nb_{2x}O_2$ ($0.05 \leqslant x \leqslant 0.30$) samples fired at 1300 °C. The linear increase of these parameters with composition confirms the formation of the expected rutile solid solutions. The increase of the a parameter is higher than the increase of the c parameter. Therefore, a distortion in the rutile structure is obtained with these solid solutions.

Fig. 2 shows the UV–V spectra in $Ni_xTi_{1-3x}B_{2x}O_2$ (B = Sb, Nb) samples. When the rutile crystalline phase is detected in samples, three absorption bands are observed at 1100–1200, 650–850 and 350–450 nm. This last value is very close to the absorption band of undoped rutile due to $Ti^{4+} \leftrightarrow O^{2-}$ charge transfer. These bands are assigned to Ni^{2+} in an octahedral site. The three spin allowed transitions: $^3A_{2g} \rightarrow {}^3T_{2g}(F)$, $^3A_{2g} \rightarrow {}^3T_{1g}(F)$ and $^3A_{2g} \rightarrow {}^3T_{1g}(P)$ generally fall within the ranges 1400–800, 900–500 and 550–370 nm respectively in octahedral systems.[19] In addition two spin forbidden bands are usually quite prominent, one, the transition to ^1E_g near the second spin allowed transition (for common systems with Dq/B near unity), and the second, primarily $^1T_{2g}$ between the second and third spin allowed band. The ^1E_g state (Dq/B≈1) lies so close to $^3T_{1g}$ that extensive mixing takes place leading to observation of a doublet band where the spin forbidden transition has stolen intensity from the spin allowed transition. Charge transfer bands about 300–500 nm obscure the third allowed transition in rutile solid solutions. Charge transfer transitions decrease in absor-

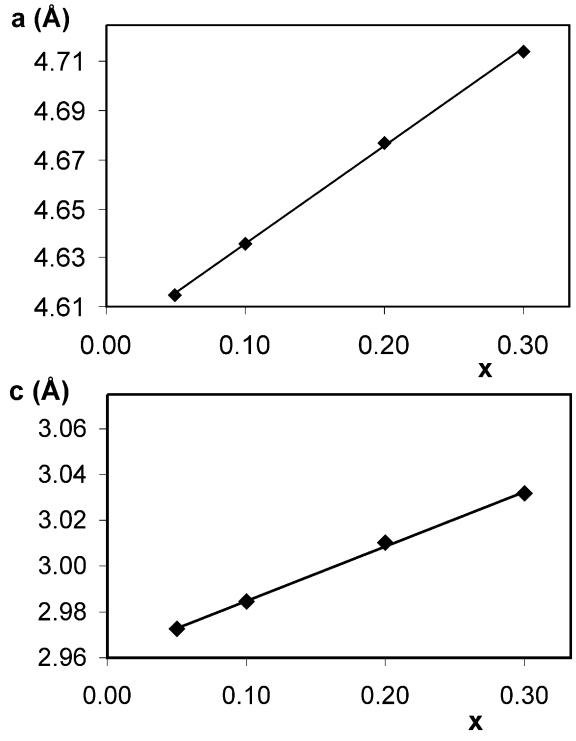

Fig. 1. Rutile unit cell parameters in $Ni_xTi_{1-3x}Nb_{2x}O_2$ ($0.05 \leqslant x \leqslant 0.30$) samples fired at 1300 °C.

bance when samples are fired at 1300 °C (Fig. 2(e)). Changes in curves are related to structural changes in samples. According with literature[13] absorption bands in $NiNb_2O_6$ (orthorhombic) are observed about 1400, 750–900 and 450–500 nm. Absorption bands in $NiSb_2O_6$ (trirutile) are observed about 1150, 650–750 and 450 nm. The smaller wavelength of transitions bands in $NiSb_2O_6$ compared with $NiNb_2O_6$ might be explained by the changes on crystal field strength (smaller mean Ni–O distances in $NiSb_2O_6$ compared with $NiNb_2O_6$). A comparison of UV–V spectra in samples with rutile, trirutile or orthorhombic structure is shown in Fig. 2(f). At 1300 °C, UV–V spectra in $Ni_xTi_{1-3x}Nb_{2x}O_2$ samples (Fig. 2(d)) changes progressively with x but orthorhombic phase is only detected when $x = 1/3$. This could be due to the progressive distortion of octahedral sites in the rutile structure when x increases.

Table 3 shows the variation of CIE L^*, a^* and b^* parameters of $Ni_xTi_{1-3x}B_{2x}O_2$ (B = Sb, Nb) samples. At 1000 °C, yellow materials are obtained when B = Sb and $x \leqslant 0.2$ or B = Nb and $0 \leqslant x \leqslant 1/3$. In $Ni_xTi_{1-3x}Nb_{2x}O_2$ rutile solid solutions ($0 \leqslant x \leqslant 0.3$) the b^* parameter (yellow amount) decreases when x increases at this temperature (1000 °C). At 1300 °C, b^* and L^* are smaller than at 1000 °C, according with location of the trans-

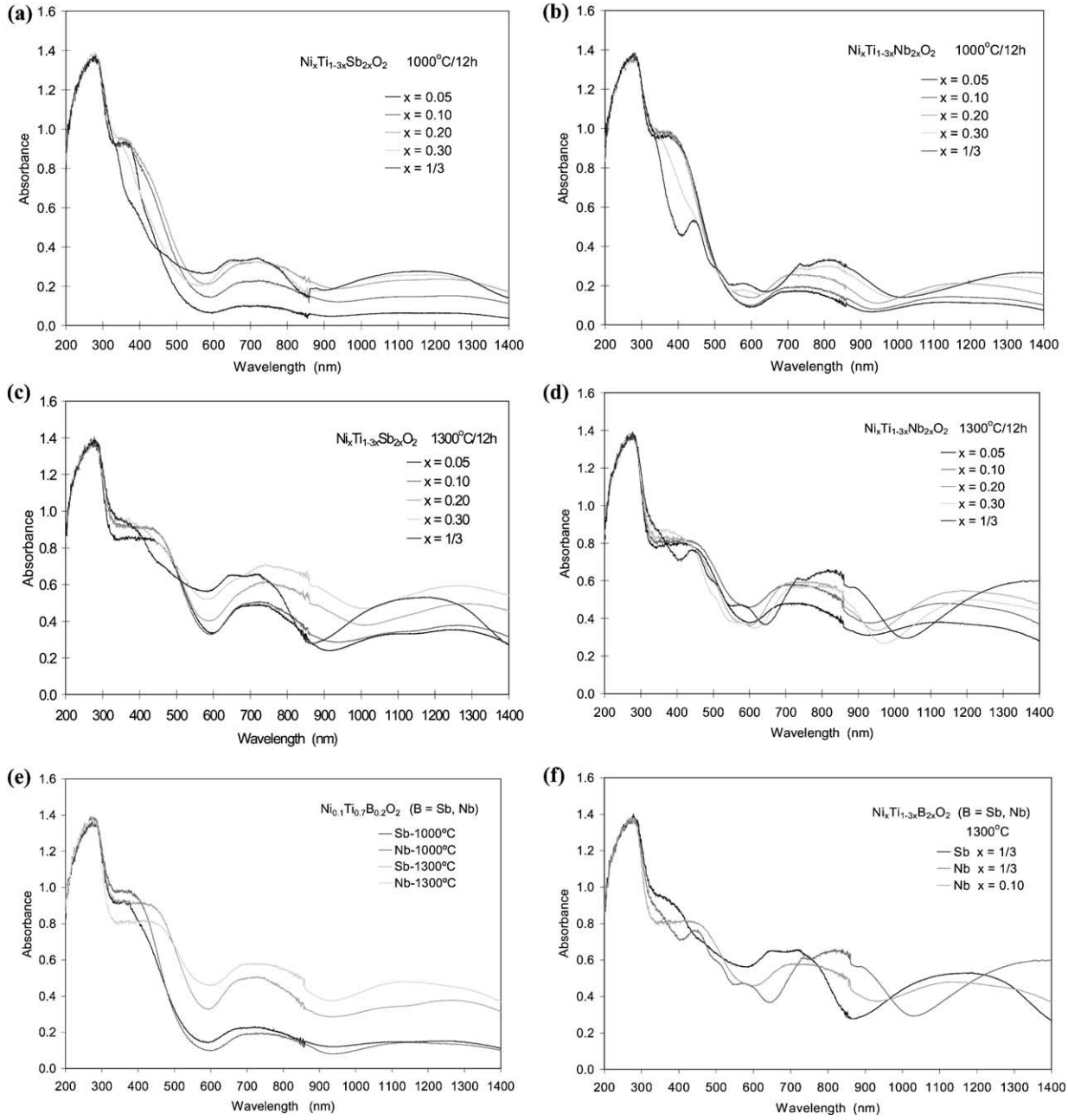

Fig. 2. UV–V spectra of $Ni_xTi_{1-3x}B_{2x}O_2$ (B = Sb, Nb) samples fired at 1000 and 1300 °C.

Table 3
Chromatic coordinates $L^*a^*b^*$ for $Ni_xTi_{1-3x}B_{2x}O_2$ samples at different temperatures

B	x	Raw sample	800 °C/12 h	1000 °C/12 h	1300 °C/12 h
Sb	0.05	$L^*=94.1$	$L^*=93.0$	$L^*=88.8$	$L^*=64.76$
		$a^*=0.0$	$a^*=-2.4$	$a^*=-4.0$	$a^*=6.56$
		$b^*=0.9$	$b^*=7.9$	$b^*=33.6$	$b^*=32.91$
Sb	0.10	$L^*=91.2$	$L^*=90.8$	$L^*=81.9$	$L^*=65.61$
		$a^*=0.1$	$a^*=-3.0$	$a^*=-2.7$	$a^*=4.56$
		$b^*=0.9$	$b^*=9.3$	$b^*=40.2$	$b^*=37.95$
Sb	0.20	$L^*=87.4$	$L^*=85.2$	$L^*=77.2$	$L^*=62.29$
		$a^*=0.3$	$a^*=-3.6$	$a^*=-4.3$	$a^*=2.34$
		$b^*=1.6$	$b^*=12.8$	$b^*=37.8$	$b^*=32.69$
Sb	0.30	$L^*=83.9$	$L^*=80.9$	$L^*=79.6$	$L^*=57.12$
		$a^*=0.6$	$a^*=-2.9$	$a^*=-9.8$	$a^*=-0.34$
		$b^*=2.4$	$b^*=13.7$	$b^*=23.0$	$b^*=20.49$
Sb	1/3	$L^*=78.8$	$L^*=76.8$	$L^*=76.3$	$L^*=56.72$
		$a^*=1.1$	$a^*=-1.4$	$a^*=-4.3$	$a^*=-3.10$
		$b^*=3.4$	$b^*=11.6$	$b^*=11.9$	$b^*=11.76$
Nb	0.05	$L^*=94.2$	$L^*=92.6$	$L^*=84.7$	$L^*=64.20$
		$a^*=0.1$	$a^*=-3.5$	$a^*=-0.5$	$a^*=4.17$
		$b^*=0.9$	$b^*=17.2$	$b^*=50.5$	$b^*=27.73$
Nb	0.10	$L^*=90.7$	$L^*=90.0$	$L^*=84.6$	$L^*=60.12$
		$a^*=-0.1$	$a^*=-3.8$	$a^*=-2.1$	$a^*=2.46$
		$b^*=0.0$	$b^*=16.0$	$b^*=49.2$	$b^*=23.14$
Nb	0.20	$L^*=85.2$	$L^*=85.8$	$L^*=82.7$	$L^*=65.50$
		$a^*=0.4$	$a^*=-4.2$	$a^*=-3.8$	$a^*=1.53$
		$b^*=1.3$	$b^*=18.7$	$b^*=43.3$	$b^*=29.23$
Nb	0.30	$L^*=83.8$	$L^*=82.7$	$L^*=82.2$	$L^*=67.53$
		$a^*=0.2$	$a^*=-4.0$	$a^*=-4.1$	$a^*=-1.57$
		$b^*=1.2$	$b^*=18.0$	$b^*=33.6$	$b^*=29.71$
Nb	1/3	$L^*=80.4$	$L^*=82.6$	$L^*=80.4$	$L^*=62.60$
		$a^*=0.4$	$a^*=-2.1$	$a^*=-2.4$	$a^*=2.63$
		$b^*=2.0$	$b^*=11.0$	$b^*=27.1$	$b^*=21.81$

mission window defined by the wings of the absorption bands in 800 and 400 regions. The optimal temperature to obtain yellow rutile solid solutions is between 1000 and 1300 °C. Compositions with $x \leqslant 0.10$ are suitable for to yellow materials. From these results, $x=0.10$ was chosen to compare results when A = Ti and A = Sn (rutile or cassiterite host matrix). In these samples ($Ni_{0.10}Ti_{0.70}Sb_{0.20}O_2$ and $Ni_{0.10}Ti_{0.70}Nb_{0.20}O_2$) rutile crystalline phase is detected by XRD. Thus, $Ni_{0.1}A_{0.7}B_{0.2}O_2$ (A = Ti, Sn; B = Sb, Nb) samples were also prepared. These samples were fired at temperatures between 1000 and 1400 °C (thermal history B) to study the crystalline phase evolution and variation of color in them.

Crystalline phase evolution with temperature in $Ni_{0.10}A_{0.70}B_{0.20}O_2$ (A = Ti, Sn; B = Sb, Nb) samples is shown in Table 4. Formation of $NiTiO_3$ was detected in the $Ni_{0.10}Ti_{0.70}Sb_{0.20}O_2$ sample at 1400 °C. When A = Sn and B = Sb, cassiterite is the only phase obtained in the 1000–1300 °C range but NiO is also detected at 1400 °C. $NiNb_2O_6$ isostructural with cassiterite was detected between 1000 and 1400 °C when A = Sn and B = Nb.

Table 5 shows cassiterite and rutile unit cell parameters obtained by the Rietveld method for $Ni_{0.10}A_{0.70}B_{0.20}O_2$ (A = Ti, Sn; B = Sb, Nb) samples fired at 1200, 1300 and 1400 °C. These unit cell parameters are in accordance with the replacement of ions proposed when solid solutions are formed and crystalline phases detected at each temperature. A progressive increase of octahedral distortion with temperature is detected if the phase composition is constant (A = Ti, B = Nb).

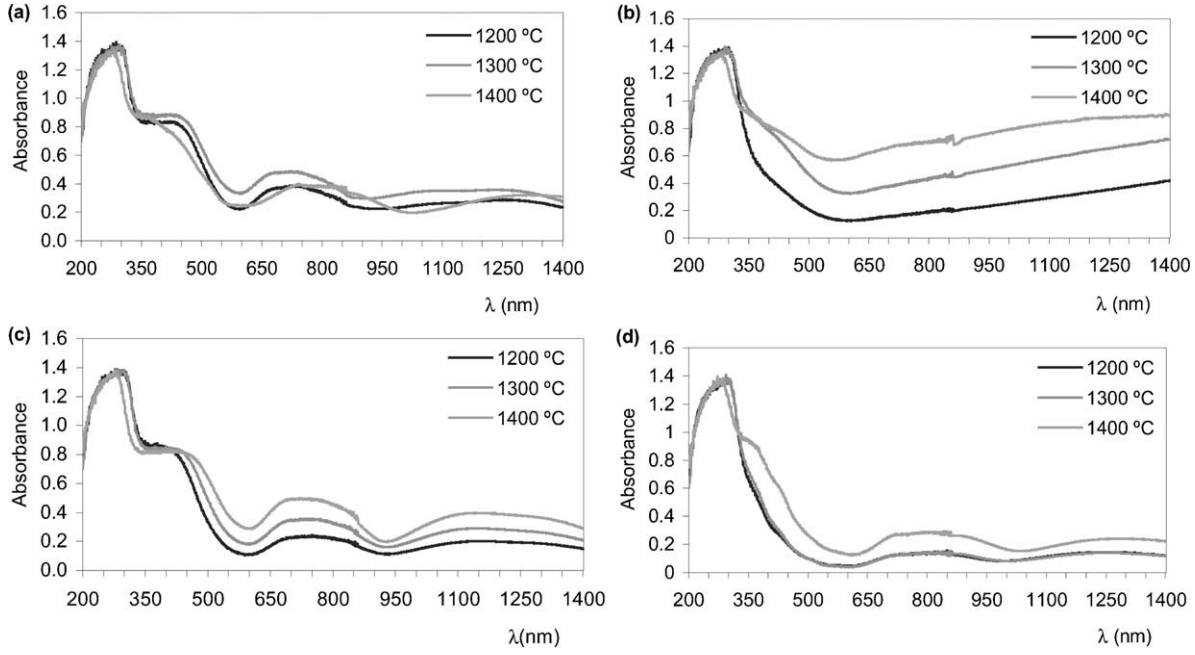

Fig. 3. UV–V spectra of $Ni_{0.1}A_{0.7}B_{0.2}O_2$ samples fired at 1200, 1300 and 1400 °C; (a) A = Ti, B = Sb; (b) A = Sn, B = Sb; (c) A = Ti, B = Nb; (d) A = Sn, B = Nb.

UV–V spectra in $Ni_{0.1}A_{0.7}B_{0.2}O_2$ (A = Ti, Sn; B = Sb, Nb) samples are shown in Fig. 3. Three absorption bands assigned to Ni^{2+} in an octahedral site are observed. Position of these bands changes with the decomposition of rutile solid solution at 1400 °C in $Ni_{0.1}Ti_{0.7}Sb_{0.2}O_2$ sample (Fig. 3(a)). The observed change in the UV–V spectrum might be due to a valency change of nickel but the volumetric increase of the unit cell as well as the octahedral distortion should correspond to the values expected on the basis of the amount of Ni and B ion and their radii. This change is in accordance with the formation of $NiTiO_3$ detected by XRD. The broad absorption in $Ni_{0.1}Sn_{0.7}Sb_{0.2}O_2$ sample (Fig. 3(c)) can be attributed to charge transfer transitions between tin and antimony ions in cassiterite solid solutions.[20] At 1400 °C, the absorbance does not decrease with segregation of NiO detected by XRD, thus Sb_2O_4–SnO_2 solid solutions with cassiterite struc-

Table 4
Crystalline phase evolution with temperature in $Ni_{0.1}A_{0.7}B_{0.2}O_2$ samples

A	B	1000 °C/12 h	1200 °C/12 h	1300 °C/12 h	1400 °C/12 h
Ti	Sb	R(s)	R(s)	R(s)	R(s), NT(w)
Ti	Nb	R(s)	R(s)	R(s)	R(s)
Sn	Sb	C(s)	C(s)	C(s)	C(s), N(vw)
Sn	Nb	C(s), HN(w), NN(w)	C(s),HN(w), NN(w)	C(s), NN(w)	C(s), NN(vw)

Crystalline phases: R = TiO_2 (rutile), C = SnO_2 (cassiterite), N = NiO, NT = $NiTiO_3$, HN = H–Nb_2O_5, NN = $NiNb_2O_6$ (tetragonal).Diffraction peak intensity: s = strong, m = medium, w = weak, vw = very weak.

Table 5
Rutile and cassiterite unit cell parameters and interatomic distances for $Ni_{0.1}A_{0.7}B_{0.2}O_2$ samples[a]

A	B	1200 °C/12 h	1300 °C/12 h	1400 °C/12 h
Ti	Sb	a = 4.6059(3)	a = 4.6069(2)	a = 4.5945(2)
		c = 2.9876(2)	c = 2.9917(1)	c = 2.9696(2)
		x (O) = 0.305(1)	x (O) = 0.300(7)	x (O) = 0.3038(8)
		M–O (×2) = 1.984(5)	M–O (×2) = 1.954(3)	M–O (×2) = 1.974(4)
		M–O (×4) = 1.962(4)	M–O (×4) = 1.984(2)	M–O (×4) = 1.957(2)
		R_p = 10.6%	R_p = 11.3%	R_p = 11.6%
		R_{wp} = 14.2%	R_{wp} = 14.6%	R_{wp} = 14.8%
		R_e = 9.4%	R_e = 10.3%	R_e = 9.8%
		R_B = 3.9%	R_B = 4.3%	R_B = 4.7%
Ti	Nb	a = 4.6327(2)	a = 4.6358(1)	a = 4.6369(2)
		c = 2.9828(1)	c = 2.9845(1)	c = 2.9855(1)
		x (O) = 0.3031(5)	x (O) = 0.3042(6)	x (O) = 0.310(1)
		M–O (×2) = 1.986(2)	M–O (×2) = 1.994(3)	M–O (×2) = 2.036(7)
		M–O (×4) = 1.972(2)	M–O (×4) = 1.968(2)	M–O (×4) = 1.942(4)
		R_p = 10.6%	R_p = 9.8%	R_p = 11.6%
		R_{wp} = 14.6%	R_{wp} = 14.0%	R_{wp} = 15.2%
		R_e = 10.1%	R_e = 9.1%	R_e = 10.5%
		R_B = 3.8%	R_B = 4.8%	R_B = 5.3%
Sn	Sb	a = 4.7248(2)	a = 4.71671(8)	a = 4.7359(1)
		c = 3.1737(2)	c = 3.16440(7)	c = 3.1845(1)
		x (O) = 0.306(1)	x (O) = 0.3041(9)	x (O) = 0.330(2)
		M–O (×2) = 2.048(6)	M–O (×2) = 2.028(4)	M–O (×2) = 2.214(8)
		M–O (×4) = 2.047(4)	M–O (×4) = 2.052(3)	M–O (×4) = 1.955(6)
		R_p = 11.3%	R_p = 11.0%	R_p = 11.7%
		R_{wp} = 14.2%	R_{wp} = 15.5%	R_{wp} = 15.8%
		R_e = 12.2%	R_e = 9.3%	R_e = 10.6%
		R_B = 3.9%	R_B = 2.9%	R_B = 5.7%
Sn	Nb	a = 4.7357(2)	a = 4.7341(2)	a = 4.7343(1)
		c = 3.1840(2)	c = 3.1791(1)	c = 3.1615(1)
		x (O) = 0.303(1)	x (O) = 0.304(1)	x (O) = 0.305(1)
		M–O (×2) = 2.029(6)	M–O (×2) = 2.036(6)	M–O (×2) = 2.040(6)
		M–O (×4) = 2.068(4)	M–O (×4) = 2.060(4)	M–O (×4) = 2.052(4)
		R_p = 9.6%	R_p = 11.4%	R_p = 11.6%
		R_{wp} = 14.1%	R_{wp} = 14.8%	R_{wp} = 14.2%
		R_e = 7.9%	R_e = 8.5%	R_e = 8.3%
		R_B = 4.2%	R_B = 5.1%	R_B = 5.3%

[a] The errors are included in parenthesis.

Table 6
Molar susceptibility (emu/mol Ni) for $Ni_{0.1}A_{0.7}B_{0.2}O_2$ samples at 294 K

A	B	1300 °C/12 h	1400 °C/12 h
Ti	Sb	0.33 10^{-2}	0.36 10^{-2}
Ti	Nb	0.2810^{-2}	0.28 10^{-2}
Sn	Sb	0.09 10^{-2}	0.04 10^{-2}
Sn	Nb	0.31 10^{-2}	0.30 10^{-2}

Table 7
Chromatic coordinates $L^*a^*b^*$ for $Ni_{0.1}A_{0.7}B_{0.2}O_2$ samples at 1200, 1300 and 1400 °C

A	B	1200 °C/12 h	1300 °C/12 h	1400 °C/12 h
Ti	Sb	$L^*=73.09$	$L^*=65.86$	$L^*=74.03$
		$a^*=3.77$	$a^*=3.86$	$a^*=1.67$
		$b^*=43.47$	$b^*=36.66$	$b^*=35.54$
Ti	Nb	$L^*=83.61$	$L^*=76.49$	$L^*=67.97$
		$a^*=-1.46$	$a^*=2.47$	$a^*=6.06$
		$b^*=49.45$	$b^*=47.02$	$b^*=36.18$
Sn	Sb	$L^*=85.96$	$L^*=70.17$	$L^*=56.98$
		$a^*=-1.63$	$a^*=-1.13$	$a^*=-3.62$
		$b^*=18.93$	$b^*=25.41$	$b^*=12.14$
Sn	Nb	$L^*=93.40$	$L^*=95.68$	$L^*=83.95$
		$a^*=-3.43$	$a^*=-3.85$	$a^*=-2.02$
		$b^*=17.95$	$b^*=19.87$	$b^*=32.32$

ture seems to be developed at this temperature in this sample.

Molar susceptibility at 294 K in $Ni_{0.1}A_{0.7}B_{0.2}O_2$ (A = Ti, Sn; B = Sb, Nb) samples (Table 6) is in accordance with the values obtained in $Ti_{3(1-x)}Ni_xM'_{2x}O_6$ (M′ = Sb, Nb) rutile solid solutions and reported by Belloch et al.[11] These results confirm the +2 oxidation state of nickel. No interactions between paramagnetic ions take place in $Ni_{0.1}Ti_{0.7}B_{0.2}O_2$ (B = Sb, Nb) and $Ni_{0.1}Sn_{0.7}Nb_{0.2}O_2$ samples. Antiferromagnetic interactions might explain the small value of molar susceptibility obtained when A = Sn and B = Sb.

CIE L^*, a^* and b^* parameters of $Ni_{0.1}A_{0.7}B_{0.2}O_2$ (A = Ti, Sn; B = Sb, Nb) samples are shown in Table 7. The variations of the b^* parameter are noteworthy and they can be explained with the occurrence of different amounts of secundary phases. When A = Ti, the b^* parameter (yellow amount) decreases with temperature. In $Ni_{0.1}Ti_{0.7}Nb_{0.2}O_2$ sample this b^* decrease can be related with the progressive increase of octahedral distortion. When A = Sn, 1300 °C (B = Sb) or 1400 °C (B = Nb) is the temperature in which b^* parameter is higher. A worse yellow color is obtained when A = Sn than when A = Ti at all temperatures. From XRD results and chromatic coordinates, $Ni_{0.1}Ti_{0.7}Nb_{0.2}O_2$ fired at 1200 °C is the best yellow material of $Ni_{0.1}A_{0.7}B_{0.2}O_2$ (A = Ti, Sn; B = Sb, Nb) samples.

From results obtained for all prepared samples, $Ni_xA_{1-3x}B_{2x}O_2$ with A = Ti, B = Nb, $x \leqslant 0.10$ and 1000 °C $\leqslant T \leqslant$ 1200 °C might be established as compositional and firing temperature ranges to obtain yellow ceramic pigments in these systems.

4. Conclusions

$Ni_xTi_{1-3x}Sb_{2x}O_2$ ($0 \leqslant x \leqslant 0.10$) and $Ni_xTi_{1-3x}Nb_{2x}O_2$ ($0 \leqslant x \leqslant 0.30$) rutile solid solutions have been obtained at 1300 °C. In these solid solutions, variation of color is related to changes in composition or temperature. Optimal yellow color is found with $x \leqslant 0.10$.

Crystalline phase evolution with temperature in $Ni_{0.10}A_{0.70}B_{0.20}O_2$ (A = Ti, Sn; B = Sb, Nb) samples shows instability of solid solutions at 1400 °C. Formation of $NiTiO_3$ in $Ni_{0.10}Ti_{0.70}Sb_{0.20}O_2$ sample is detected at 1400 °C. When A = Sn and B = Sb, cassiterite is the only phase obtained in the 1000–1300 °C temperature range, but NiO is also detected at 1400 °C. When A = Sn and B = Nb, $NiNb_2O_6$ isostructural with cassiterite is detected between 1000 and 1400 °C.

$Ni_xA_{1-3x}B_{2x}O_2$ with A = Ti, B = Nb, $x \leqslant 0.10$ and 1000 °C $\leqslant T \leqslant$ 1200 °C might be established as compositional and firing temperature ranges to obtain yellow ceramic pigments in these systems.

Acknowledgements

We gratefully acknowledge the financial support given by M C Y T, MAT 2001-3771 project.

References

1. Badenes, J. A., Vicent, J. B., Llusar, M., Tena, M. A. and Monrós, G., The nature of Pr–$ZrSiO_4$ yellow ceramic pigment. *J. Mater. Sci.*, 2002, **37**, 1413–1420.
2. Monrós, G., Carda, J., Tena, M. A., Escribano, P. and Alarcón, J., Synthesis of ZrO_2–V_2O_5 Pigments by sol-gel methods. *Br. Ceram. Trans. J.*, 1991, **90**, 157–160.
3. Ren, F., Ishida, S. and Takeuchi, N., Color and vanadium valency in V-doped ZrO_2. *J. Am. Ceram. Soc.*, 1993, **76**, 1825–1831.
4. Fujiyoshi, K. and Yokoyama, H., *Chemical State of Vanadium in Tin-Based Yellow Pigment*, 1993, **76**, 981–986.
5. Loridant, S., Determination of the maximum vanadium oxide coverage on SnO_2 with a high surface area by Raman spectroscopy. *J. Phys. Chem. B*, 2002, **106**, 13273–13279.
6. Campbell, I., Lead and cadmium free glasses and frits. *Glass Technology*, 1998, **39**, 38–41.
7. Ishida, S., Ren, F. and Takeuchi, N., New yellow ceramic pigment based on codoping pyrochlore $Y_2Ti_2O_7$ with V^{5+} and Ca^{2+}. *J. Am. Ceram. Soc.*, 1993, **76**, 2644–2648.
8. Estrada, C. L., Torres-Gonzalez, L. C., Fuentes, A. F., Torres-Martinez, L. M. and Quintana, P., Synthesis of new vanadium cordierite pigment by sol-gel processing. *Br. Ceram. Trans.*, 2000, **99**, 67–71.
9. DCMA Classification and Chemical description of the Mixed Metal Oxide Inorganic Coloured Pigments, *Metal Oxides and*

Ceramics Colors Subcommitee, 2ª ed. Dry Color Manufacturer's Ass, Washington, DC, 1982.
10. Ramos, E., Veiga, M. L., Fernández, F., Sáez-Puche, R. and Pico, C., Synthesis, structural characterization, and two-dimensional antiferromagnetic ordering for the oxides $Ti_{3(1-x)}Ni_xSb_{2x}O_6$ ($1.0 \geqslant x \geqslant 0.6$). *J. Solid State Chem.*, 1991, **91**, 113–120.
11. Belloch, J. M., Isasi, J., López, M. L., Veiga, M. L. and Pico, C., Synthesis, characterization and semiconducting properties of solid solutions with rutile structure. *Mater. Research Bull.*, 1994, **29**, 861–869.
12. Belloch, J. M., Isasi, J., López, M. L., Veiga, M. L., Pico, C., Fischer, S. and Gopel, W., Solid Solutions with rutile structure: electronic behaviour and ultraviolet photoelectron spectrometry study. *J. Mater. Sci.*, 1996, **31**, 6609–6614.
13. Rossman, G. R., Shannon, R. D. and Waring, R. K., Origin of the yellow color of complex nickel oxides. *J. Solid State Chem.*, 1981, **39**, 277–287.
14. Czajkowski, W. and Kraska, J., Studies on the dependence between structure and color of some nickel-complexed pigments, derivates of 2,3-dioximes of 2,3-dioxobutanoic acid arylides. *Polish J. Of Chem.*, 1984, **58**, 479–485.
15. Kuchen, W., Mootz, D., Poll, W. and Stephan, R., Relation between colour and crystal structure in two isomeric nickel complexes. *Acta Crystallographica section A*, 1984, **40**, C309.
16. Croft, G. and Fuller, M. J., Crystalline oxidic solid solutions of Tin(IV) and Titanium(IV), their coloration by and thermal reaction with some metal ions. Part 1: The rutile $Sn_xTi_{(1-x)}O_2$ system and its interaction with V(V), Cr(III), Cr(VI), Mn(II), Fe(III), Co(II), Ni(II), Cu(II) and Sb(III). *Trans. J. Br. Ceram. Soc.*, 1979, **78**, 52–56.
17. J. Rodriguez-Carvajal: FULLPROF computer program, wfp2ks.exe (May2001-LLB-JRC), Laboratoire Leon Brillouin (CEA-CNRS), France (2001).
18. Commission Internationale del'Eclairage, ''Recommendations on Uniform Color Spaces, Color Difference Equations, Phychometrics Color Terms'', Supplement No. 2 of CIE Publication No. 15 (E1-1.31) 1971 (Bureau Central de la CIE, Paris, 1978).
19. Lever, A. B. P., *Inorganic Electronic Spectroscopy*, (second ed.). Elsevier Science B.V, The Netherlands, 1977.
20. Sala, F. and Trifiró, F., Oxidation catalysts based on Tin–Antimony oxides. *J Catalysis*, 1974, **34**, 68–78.